A Fluorescence Spectroscopy Study on the Interactions of the TAT-PTD Peptide with Model Lipid Membranes

Venkataswarup Tiriveedhi and Peter Butko*

Department of Chemistry and Biochemistry, University of Southern Mississippi, Hattiesburg, Mississippi 39406

Received December 7, 2006; Revised Manuscript Received February 3, 2007

ABSTRACT: Protein-transduction domains (PTDs) have been shown to translocate into and through the living cells in a rapid manner by an as yet unknown mechanism. Regardless of the mechanism of translocation, the first necessary step must be binding of the PTD peptide to the surface of the lipid membrane. We used fluorescence spectroscopy to study the interaction between PTD of the HIV-1 Tat protein (TAT-PTD; residues 47−60 of Tat, fluorescently labeled with tryptophan) and the lipid bilayer labeled with various fluorescence membrane probes. The TAT-PTD tryptophan exhibited a decrease in fluorescence intensity and an increase in anisotropy upon interaction with lipid bilayers. The fluorescence changes were linearly proportional to the density of negative charge in the membrane. Kinetic analysis of the interaction showed two apparent dissociation constants. The value of one dissociation constant (K_{d1} = 2.6 ± 0.6 μM), which accounted for 24% of the interaction, was found to be independent of the negative charge density, suggesting its nonelectrostatic nature. The value of the second dissociation constant (K_{d2}), which accounted for 76% of the interaction, decreased linearly from 610 ± 150 to 130 ± 30 μM with an increase in negative charge density from 0 to 25 mol %, suggesting this interaction is electrostatic in nature. Even though the binding was predominantly electrostatic, it could not be reversed by high salt, indicating the presence of a second, irreversible, step in the interaction with lipid. When TAT-PTD was bound to lipid vesicles labeled with 1-(4-trimethylammoniumphenyl)-6-phenyl-1,3,5-hexatriene (TMA-DPH), fluorescence resonance energy transfer between the tryptophan and the probe occurred at a distance of 3.4 nm. No change in fluorescence anisotropy of either TMA-DPH or DPH was observed upon the interaction with TAT-PTD, indicating no significant disruption or perturbation of the lipid bilayer by the peptide. TAT-PTD did not cause dissipation of membrane potential (165 mV, negative inside). Inclusion of 3% pyrene-labeled phosphatidylglycerol (pyrene-PG) in the membrane revealed that TAT-PTD preferentially bound to the membrane in the liquid state. We conclude that membrane fluidity is an important physicochemical parameter, which may regulate binding of TAT-PTD to the membrane.

Over the past several years, certain peptides and proteins have been shown to penetrate the cell membrane and enter the cell by a process called protein transduction and to reach the nucleus while retaining their normal biological activity (*1*−*6*). The corresponding amino acid sequences are called protein-transduction domains (PTDs)[1] and the peptides themselves cell-penetrating peptides (CPPs) or Trojan horse peptides (*7*−*11*). Some naturally occurring CPPs are derived from HIV-1 TAT (trans activator of transcription) protein, Ant P penetratin of *Drosophila* antennapedia homeoprotein, vp22 from Herpes virus, or the flock house virus coat protein. Synthetic CPPs include transportan, a synthetic peptide adapted from the neuropeptide galanin, or SynB peptide derived from the antimicrobial protein protegrin (*8*, *12*, *13*). CPPs have been shown to internalize by a variety of primary cells, such as rat brain and rat spinal cord, calf aorta, and other cell lines (*14*, *15*). No specialized cultivating procedures were needed for the internalization (*16*, *17*). CPPs were shown to rapidly internalize into the cell in an apparently energy independent manner [it was observed even at 4 °C, when all the metabolism ceases, and their uptake seemed unaffected by inhibitors of the classical endocytosis pathway (*14*, *18*−*20*)], but it turned out more recently that artifacts due to cell fixation and insufficient removal of surface-bound (as opposed to truly internalized) peptides might have significantly contributed to those results (*6*). Internalization is reported to occur with D and L stereoisomers of the peptides (*18*), which is used to support the notion that no receptor is required for the process.

After the promising claims of TAT-PTD translocation across membranes in live cells (*14*, *21*) in a so-called energy-independent manner, more recent evidence has established

* To whom correspondence should be addressed. Phone: (601) 266-6044 (office) and (601) 266-6456 (lab). Fax: (601) 266-6075. E-mail: peter.butko@usm.edu.

[1] Abbreviations: CPP, cell-penetrating peptide; DMPC, 1,2-dimyristoyl-*sn*-glycero-3-phosphocholine; DMPG, 1,2-dimyristoyl-*sn*-glycero-3-[phospho-*rac*-(1-glycerol)]; DPPS, dipalmitoylphosphatidylserine; $DiSC_3(5)$, 3,3′-dipropylthiadicarbocyanine iodide; DPH, 1-(4-trimethylammoniumphenyl)-6-phenyl-1,3,5-hexatriene; PC, L-α-phosphatidylcholine; PG, L-α-phosphatidylglycerol; FRET, fluorescence resonance energy transfer; HEPES, 4-(2-hydroxyethyl)-1-piperazineethanesulfonic acid; LUV, large unilamellar vesicles; NATA, *N*-acetyl tryptophanamide; pyrene-PG, 1-hexadecanoyl-2-(1-pyrenedecanoyl)-*sn*-glycero-3-phosphoglycerol; PTD, protein-transduction domain; SUV, small unilamellar vesicles, with a diameter of ∼25 nm; TAT, transacting activator of transcription; TMA-DPH, 1-(4-trimethylammoniumphenyl)-6-phenyl-1,3,5-hexatriene.

10.1021/bi602527t CCC: $37.00
Published on Web 03/06/2007

that the intracellular entry of TAT PTD does not occur at low temperatures (*6*). A consensus that the most plausible mechanism appears to be classical or nonclassical endocytosis is developing (*6*, *22*, *23*), although nonendocytotic pathways are also considered (*24*). Because of the variability in their individual structures, there is no reason to expect a single unified mode of action of CPPs (*25*, *26*).

Despite questions about their mechanism, CPPs have a great potential in biotechnology applications. They are able to carry along wide variety of covalently attached molecules, such as enzymes with molecular masses of up to 120 kDa, liposomes with a diameter of 200 nm, 40 nm magnetic nanoparticle beads, and DNA phages (*27*−*30*). Thus, CPPs are capable of improving or enabling uptake and possible nuclear targeting of biologically active large molecules, which makes them a desirable candidate for intracellular drug delivery and rapid nonviral gene transfer systems.

Work in our laboratory focused on the CPP derived from HIV-1 Tat protein (trans activator of transcription), one of the 15 proteins encoded by HIV-1 virus (*31*). A fragment of Tat protein comprising the basic region has been shown to internalize into cells in culture and is therefore called Tat protein transduction domain (TAT-PTD) (*14*, *32*). However, the exact mechanism of internalization is yet unknown.

The internalization seems to be passive, but for a peptide with eight positive charges within just 14 amino acid residues, the energy barrier in the hydrophobic core of the lipid bilayer would be very high. Recent theories of complexation with glycoproteins (*33*, *34*) or lipid molecules are yet to be proven beyond controversy. Regardless of the mechanism of translocation, the first necessary step must be binding of the PTD peptide to the surface of the lipid membrane, and this is the topic of our work. Herein, we focus on this initial interaction of TAT-PTD with a bare lipid bilayer (i.e., in the absence of other molecules, such as proteins or carbohydrates). While cell cultures, tissues, and whole organisms are good systems for showing the action of CPPs under conditions close to in vivo conditions, the use of a simple, well-defined, and well-understood model system provides a better opportunity to reveal the molecular mechanism of protein transduction. Two main characteristics that distinguish our model system from real cells in tissue are the absence of extracellular matrix proteoglycans and the random distribution of acidic phospholipids between the two leaflets of the membrane. Despite this simplification, it is believed that our findings are of interest and our results have some biological relevance. Using fluorescence spectroscopy, we determined apparent binding constants, inferred the location of the bound peptide with respect to the bilayer, and studied the effects of salts, membrane potential, and membrane fluidity on the binding.

MATERIALS AND METHODS

Materials. A fluorescent analogue of TAT-PTD with a tyrosine replaced with tryptophan (H_3N^+-YGRKKRRQRRRPPQ-COO^-), 99.9% pure, was obtained from New England Peptide, Inc. (Gardner, MA). *N*-Acetyltryptophanamide (NATA) and lipid egg PC (L-α-phosphatidylcholine) were obtained from Sigma-Aldrich (St. Louis, MO). Lipids egg PG (L-α-phosphatidylglycerol), DPPS (dipalmitoylphosphatidylserine), DMPC (1,2-dimyristoyl-*sn*-glycero-3-phosphocholine, sodium salt), and DMPG {1,2-dimyristoyl-*sn*-glycero-3-[phospho-*rac*-(1-glycerol)], sodium salt} were obtained from Avanti Polar Lipids **(**Alabaster, AL). The ionophore valinomycin and the fluorescence probes $DiSC_3$-(5) (3,3′-dipropylthiadicarbocyanine iodide), TMA-DPH [1-(4-trimethylammoniumphenyl)-6-phenyl-1,3,5-hexatriene], and DPH (1,6-diphenyl-1,3,5-hexatriene) and pyrene-PG [1-hexadecanoyl-2-(1-pyrenedecanoyl)-*sn*-glycero-3-phosphoglycerol] were obtained from Invitrogen-Molecular Probes (Carlsbad, CA). All buffers and salts were from either Fisher Scientific (Pittsburgh, PA) or VWR (Atlanta, GA) and used at the highest available purity.

Buffers containing 10 mM HEPES and 150 mM NaCl (for NaCl-HEPES buffer) or 150 mM KCl (for KCl-HEPES buffer) (pH 7.4) were prepared.

Vesicle Preparation. Small unilamellar vesicles (SUV) were prepared by sonication (*35*). Desired amounts of lipids were dissolved in chloroform and dried under a stream of nitrogen. The resulting dry thin film was hydrated in 0.5 mL of buffer, so the stock concentration of lipid was 13 mM. This lipid suspension was sonicated for 30 min at 4 °C with a model 300 sonic dismembrator from Fisher Scientific. Large unilamellar vesicles (LUV) were obtained by extrusion, using a LiposoFast extruder (Avestin, Inc., Ottawa, ON) with two 100 nm polycarbonate membranes (Whatman Nucleopore, Clifton, NJ) after the hydrated lipid had been frozen and thawed five times (*36*).

Fluorescence and Absorption Spectroscopy. Fluorescence measurements were performed with an ISS (Champaign, IL) K2 fluorometer equipped with a xenon lamp, variable slits, and a microprocessor-controlled photomultiplier. The samples were measured in 1 cm × 1 cm quartz cuvettes. The excitation and emission wavelengths were 280 and 360 nm for tryptophan fluorescence, 645 and 675 nm for $DiSC_3$(5), 340 and 400 nm for monomer (475 nm for excimer) for pyrene, and 355 and 430 nm for TMADPH and DPH, respectively. When excitation was in the UV region, a 305 nm filter placed on the emission side was used to reduce light scattering from the lipid. Concentrations of the peptide and fluorophores were determined by using a JASCO (Easton, MD) V-530 UV spectrophotometer. Molar extinction coefficients were 5600 cm^{-1} M^{-1} for tryptophan, 75 000 cm^{-1} M^{-1} for TMADPH, 88 000 cm^{-1} M^{-1} for DPH, and 258 000 cm^{-1} M^{-1} for $DiSC_3$(5). The same spectrophotometer was used to record absorption spectra of fluorescently labeled lipid vesicles used in FRET measurements.

Titrations of TAT-PTD with SUV, carried out at room temperature, were repeated five times. The data were corrected for dilution and analyzed using Microcal Origin 7.0 (Microcal Software, Northampton, MA). Binding of TAT-PTD to the lipid vesicles was evaluated from the decrease in fluoresence intensity at 360 nm. The data were fitted with double hyperbola using eq 1:

$$F = 1 - f_1 x/(K_{d1} + x) - f_2 x/(K_{d2} + x) \qquad (1)$$

where F is the fluorescence intensity, normalized to 1 in the absence of lipid, x is the concentration of lipid, f_1 is the fraction of binding with the apparent dissociation constant K_{d1}, and f_2 is the fraction of binding with the apparent dissociation constant K_{d2}.

To assess the TAT-PTD-induced aggregation of negatively charged lipids in the membrane, SUV were prepared with 3% pyrene-PG in 3:1 DMPC/DMPG SUV. Pyrene fluorescence was measured in the presence and absence of 8 μM TAT-PTD with an excitation wavelength of 340 nm. The excimer:monomer ratio was taken as the ratio of intensities at 475 and 397 nm.

To measure the effects of membrane fluidity, SUV were prepared with 3:1 DMPC/DMPG SUV. Titrations with TAT-PTD were carried out at 7, 17, 27, and 37 °C. The temperature was maintained within 0.1 °C using the Neslab RTE-111 circulating bath (Thermoneslab, Portsmouth, NH). The binding of TAT-PTD to the lipid vesicles was evaluated via the fluorescence intensity at 360 nm.

Fluorescence anisotropy was measured with the same fluorometer in the L format with the Glan-Thomson prism polarizers placed in the excitation and emission path. Data were collected in five individual measurements, each with 30 determinations.

Fluorescence resonance energy transfer (FRET) was also assessed with the same fluorometer. TAT-PTD was titrated with SUV labeled with 2% TMADPH or DPH. The efficieny E of energy transfer between the two fluorophores was calculated using eq 2 (*37*):

$$E = A_A(\lambda_D)/A_D(\lambda_D)[I_{AD}(\lambda_D)/I_A(\lambda_D) - 1] \quad (2)$$

where $A_A(\lambda_D)$ is the absorbance of the acceptor at the donor excitation wavelength, $A_D(\lambda_D)$ is the absorbance of the donor at its excitation wavelength, $I_{AD}(\lambda_D)$ is the fluorescence intensity of the acceptor excited at the donor wavelength in the presence of the donor, and $I_A(\lambda_D)$ is the fluorescence intensity of the acceptor excited at the donor wavelength in the absence of the donor. The distance R between the donor and acceptor was calculated from the efficiency E using eq 3 (*37*):

$$R = R_o(1/E - 1)^{1/6} \quad (3)$$

where R_o, the Forster radius, is the distance between the donor and acceptor at which there is a 50% transfer of energy. The orientation factor κ^2 was implicitly assumed to be $^2/_3$.

Fluorescence Quenching. TAT-PTD was maintained at 2 μM in the NaCl-HEPES buffer. Later, 9.6 μM LUV or SUV (separately) with 25% negatively charge lipid were added, and tryptophan fluorescence was measured at increasing concentrations of acrylamide or iodide (up to 0.8 M). The same set of experiments was also carried out with NATA as a control. The data were analyzed using the Stern−Volmer equation (*38*), eq 4, with the intrinsic protein fluorescence multiplied by the factor $10^{\epsilon[Q]/2}$ to correct for the acrylamide inner filter effect, using an extinction coefficient ϵ of 4.3 cm^{-1} M^{-1} for acrylamide at 280 nm (*39*):

$$F_0/F = 1 + K_{SV}[Q] \quad (4)$$

where F_0/F is the ratio of unquenched and quenched fluorescence intensities, [Q] is the molar concentration of the quencher, and K_{SV} is the Stern−Volmer constant.

Membrane Potential Dissipation. LUV were prepared with KCl-HEPES buffer and stored in the same manner described earlier. An aliquot of the LUV stock (final concentration of 4 μM) was placed in the NaCl-HEPES buffer, and 250 nM $DiSC_3(5)$ was added. $DiSC_3(5)$ is a slow-reponse membrane potential probe, whose fluorescence is quenched in the presence of the membrane potential (*40*). The potassium diffusion potential (negative inside) across the membrane was formed when the potassium ionophore valinomycin (2.25 nM) was added to the cuvette, The value of the membrane potential was adjusted as needed with the addition of the potassium buffer to the external environment according to the Nernst equation (eq 5) (*41*):

$$\Delta\psi = RT/(ZF)\ln(C_{in}/C_{out}) \quad (5)$$

where $\Delta\psi$ is the membrane potential, R is the gas constant, T is the absolute temperature, C is the concentration of potassium ions, Z is the charge or valence of the transported ion, and F is the Faraday constant.

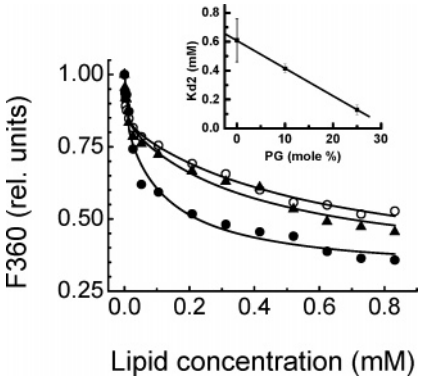

FIGURE 1: Titration of TAT-PTD with SUV with different contents of negatively charged lipids: (○) 0% PG, (▲) 10% PG, and (●) 25% PG. The inset shows the apparent dissociation constant K_{d2} as a function of PG concentration (mole percent).

RESULTS

Titration of TAT-PTD with Lipid. Titration of TAT-PTD with pure PC SUV resulted in a gradual decrease in the peptide's fluorescence (Figure 1), which was used to quantify the binding. Curve fitting with eq 1 revealed that double hyperbola fits the data the best (reduced χ^2 values of 0.00011 for 0%, 0.00059 for 10%, and 0.00144 for 25% negative charge; χ^2 values for single-hyperbola fits were 1 order of magnitude greater). For pure PC SUV, two apparent dissociation constants were observed: a K_{d1} of 2.6 ± 0.6 μM accounted for 24% of the extent of binding, and a K_{d2} of 610 ± 150 μM accounted for 76% of the interaction. When the titration was repeated with SUV containing 10% negatively charged lipid egg PG, the values of K_{d1} and the two fractions remained unchanged but the value of the second dissociation constant K_{d2} decreased to 420 ± 30 μM. Increasing the concentration of egg PG in the membrane to 25% resulted in a further decrease in K_{d2} to 130 ± 30 μM. The value of K_{d2} decreased linearly with an increase in density of negative charge in the membrane (Figure 1, inset). No lipid-induced shift in the tryptophan fluorescence spectrum was observed in either of the titrations.

It is reasonable to assume that the electrostatic binding of TAT-PTD occurs via simultaneous binding to eight negative charges in the membrane. This interaction, which would effectively neutralize the TAT-PTD molecule, requires that eight negatively charged lipid molecules move close to each

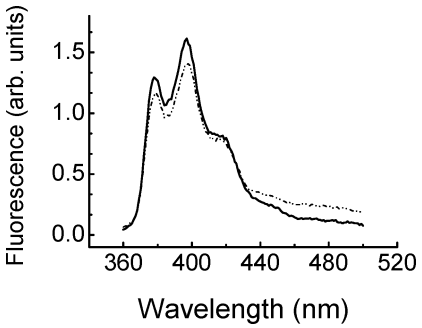

FIGURE 2: Interaction of TAT-PTD with pyrene-PG/DMPC/DMPG (3:75:22) SUV: (—) lipid only and (•••) lipid with TAT-PTD.

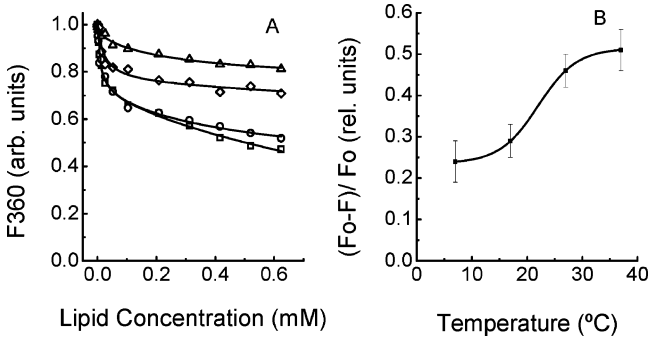

FIGURE 3: (A) Titration of TAT-PTD with 3:1 DMPC/DMPG SUV at 7 (△), 17 (◇), 27 (○), and 37 °C (□). (B) Effect of temperature on the binding of TAT-PTD to DMPC/DMPG SUV.

other in space. We tested whether indeed TAT-PTD induced selective aggregation of the negatively charged lipid by including in the membrane PG labeled with pyrene. Pyrene aggregation is marked in the fluorescence spectrum by the appearance of a broad excimer emission peak at 475 nm. The fluorescence ratio F_{475}/F_{397} is taken as a measure of the excimer:monomer concentration ratio. Figure 2 shows the spectra of DMPC/DMPG (3:1) SUV labeled with 3% pyrene-PG in the presence and absence of TAT-PTD. The presence of the peptide clearly caused a decrease in the pyrene monomer fluorescence (the region between 370 and 400 nm) and a concomitant increase in the excimer fluorescence (at ~475 nm). The F_{475}/F_{397} ratio was 0.077 and 0.166 in the absence and presence of TAT-PTD, respectively. Thus, TAT-PTD binding caused a greater than 100% increase in the excimer:monomer ratio, which proves the selective aggregation of pyrene-PG upon TAT-PTD binding.

Effect of Membrane Fluidity. To study the effect of membrane fluidity on peptide binding, we carried out titrations of TAT-PTD with SUV prepared with 3:1 DMPC/DMPG SUV. Chemically defined lipids DMPC and DMPG were used instead of egg PC and egg PG because the former lipids have a sharp phase transition temperature between the gel and liquid-crystal states. Below 23 °C, these lipids are in the gel state, characterized by low fluidity and slow lateral and rotational diffusion, and above that temperature, they are in the liquid-crystal state, marked with a high fluidity and fast diffusion (*42*, *43*). The lipid-induced changes in TAT-PTD greatly increased at higher temperatures, when the membrane was fluid, as reflected in the greater fluorescence change (Figure 3).

Effect of Salt. When the titration of TAT-PTD with 25% negatively charged lipid was performed in the presence of 2 M NaCl, we noticed a smaller decrease in fluorescence,

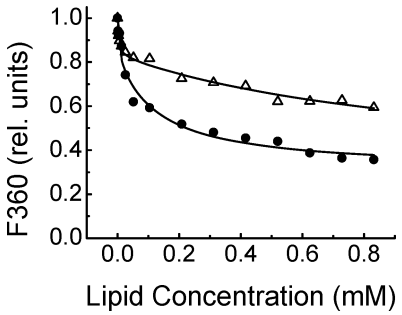

FIGURE 4: Effect of 2 M NaCl on TAT-PTD binding (△) in the presence of salt and (●) in the absence of salt.

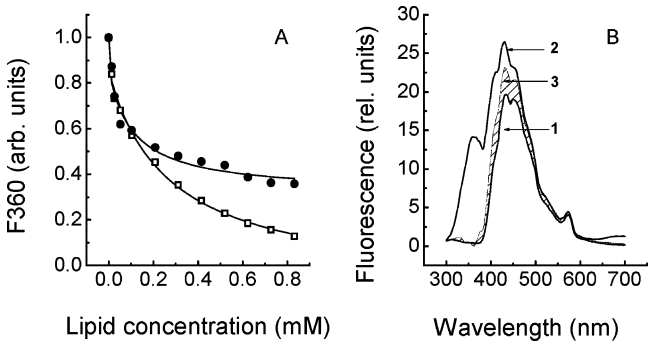

FIGURE 5: (A) Titration of TAT-PTD with 25% PG SUV labeled with 2% TMA-DPH (□) and unlabeled (●). (B) FRET between tryptophan and TMA-DPH: TMA-DPH SUV (1) excited at 280 nm, (2) after addition of TAT-PTD, and (3) after subtraction of the peptide fluorescence. The corss-hatched area shows energy transfer, after subtraction of the TMA-DPH fluorescence (spectrum 1) due to direct excitation of the probe with 280 nm light.

compared with a similar plot at a low salt concentration (Figure 4), but when the salt was added after the lipid, the tryptophan fluorescence did not change (data not shown).

FRET. When TAT-PTD was titrated with the lipid labeled with 2% TMA-DPH, a greater decrease in the tryptophan fluorescence was noticed than with the unlabeled lipid, as shown in Figure 5A. The additional quenching is attributed to the transfer of energy from tryptophan to TMA-DPH, which is more rigorously documented in Figure 5B. These data allowed for calculation of the distance between the tryptophan of TAT-PTD and TMA-DPH, whose charged head group anchors the fluorophore moiety close to the membrane interface. The efficiency of energy transfer was determined using eq 2, and the distance between the two fluorophores was calculated using eq 3. We observed an energy transfer efficiency of 50%, and therefore, the distance between the two fluorophores is 3.4 nm, the value of R_o for the tryptophan−TMA-DPH pair. In contrast with TMA-DPH, inclusion of 2% DPH in the membrane did not cause an additional decrease in the TAT-PTD fluorescence (data not shown). Within the limits of sensitivity of our instrument, there was no appreciable transfer of energy to DPH, which partitions deeper in the hydrophobic core of the lipid bilayer.

The fluorescence anisotropy of TAT-PTD was measured in the presence and absence of the lipid (Figure 6). The steady-state anisotropy of the TAT-PTD tryptophan in the buffer was −0.008 ± 0.002. Once SUV made of a neutral lipid had bound, the value increased to 0.045 ± 0.002, whereas with SUV that included a 25% negatively charged lipid, the anisotropy increased to 0.088 ± 0.002. To study the possible peptide-induced changes in the lipid order in

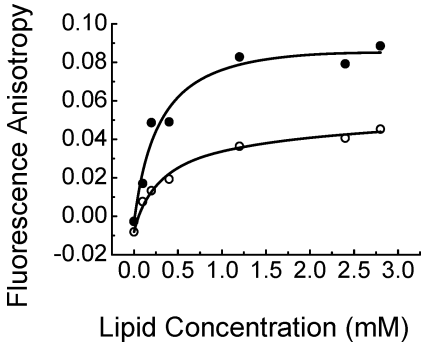

FIGURE 6: Fluorescence anisotropy change upon interaction of TAT-PTD with different lipids: (○) 0% PG and (●) 25% PG.

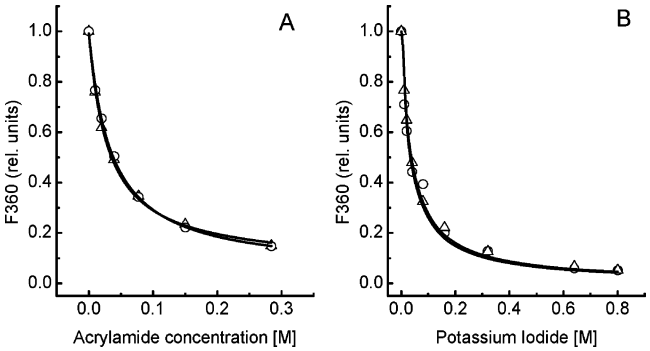

FIGURE 7: (A) Fluorescence quenching of TAT-PTD with acrylamide, in the presence and absence of lipid. (B) Fluorescence quenching of TAT-PTD by potassium iodide (○) in the absence of lipid and (△) in the presence of lipid (25% PG).

the bilayer during the peptide−lipid interaction, the membranes were labeled with the lipophilic probes DPH and TMA-DPH and the anisotropy of their fluorescence was measured. The values were 0.12 ± 0.003 and 0.225 ± 0.004 for DPH and TMA-DPH, respectively, and they did not change upon binding of TAT-PTD.

Fluorescence Quenching. The localization with respect to the membrane of the N-terminal tryptophan residue of the membrane-bound TAT-PTD can be inferred from fluorescence quenching data. Acrylamide appeared to quench the TAT-PTD fluorescence completely both in solution and when bound to the membrane (Figure 7A). Quenching of the water-soluble tryptophan derivative NATA produced exactly the same pattern (data not shown). The values of the Stern−Volmer quenching constant were 28 ± 2 and 32 ± 3 M^{-1} for TAT-PTD in the absence and presence of SUV with 25% PG, respectively. Acrylamide can to some extent partition in nonpolar environments (*44*); therefore, we repeated the quenching experiments with iodide, which, being an anion, selectively quenches fluorophores exposed to the aqueous phase. The results were the same as with acrylamide: KI completely quenched the tryptophan fluorescence both in the absence and in the presence of SUV with 25% PG. The values of the Stern−Volmer quenching constant were 26 ± 1 and 29 ± 1 M^{-1}, respectively.

Membrane Potential. To study the effect of membrane potential on the interaction of TAT-PTD with a lipid bilayer, we created an in vitro membrane potential as described in Materials and Methods. Experiments were conducted with both 0 and 25% PG LUV. In either experiment, we noticed no dissipation of membrane potential upon addition of TAT-PTD (results with 25% PG LUV are shown in Figure 8). In another experiment, we tested the possible effect of membrane potential on binding of TAT-PTD to the membrane. We observed no changes in the fluorescence of the membrane-bound peptide upon formation of a membrane potential (data not shown).

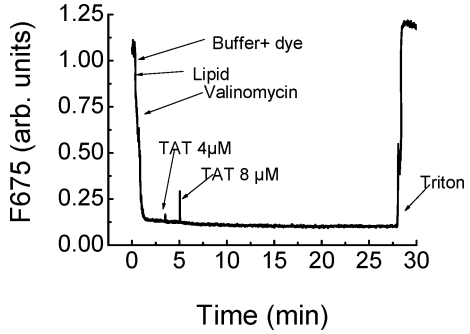

FIGURE 8: Effect of TAT-PTD on membrane potential (165 mV, negative inside) in 25% PG LUV.

DISCUSSION

The mechanism of penetration of TAT-PTD through the lipid bilayer is not known, although current evidence favors endocytosis (*6*, *22*, *23*). Regardless of the nature of subsequent events, the first necessary step for TAT-PTD penetration must be binding to the surface of the membrane. We studied this initial step using biophysical techniques with the aim of gaining quantitative insight into the process and using the model system of pure lipid vesicles, which has a limited number of variables and is better defined and controlled than live cells. The use of the model system has allowed us to characterize the membrane interaction of TAT-PTD as a function of physicochemical properties of the lipid bilayer.

Even though there were some early reports raising the possibility of specific cell surface receptors for TAT protein (*45*, *46*), experiments with L- and D-enantiomeric peptides of the CPP penetratin (*18*) do not favor the idea of CPPs binding to a specific receptor. Indeed, the high positive charge on TAT-PTD almost predestines it to bind nonspecifically to any negatively charged molecule or organelle, including the lipid membrane. Binding of TAT-PTD to glycosaminoglycans, components of the extracellular matrix (*33*, *34*, *47*), has been considered biologically relevant for CPPs binding to, and penetration across, the cell membrane. The issue will be addressed in a separate manuscript (in preparation), but our preliminary data as well as recent data from other laboratories (*48*, *49*) do not support this hypothesis.

Effect of Lipid Composition. Our data indicate that the interaction of TAT-PTD with the lipid bilayer involves two phases. With the pure PC SUV, 24% of the binding occurred with an apparent dissociation constant K_{d1} of 2.6 ± 0.6 μM, while the remaining 76% of the interaction had an apparent dissociation constant K_{d2} of 610 ± 150 μM. Increasing the density of the negative charge in the membrane caused a significant decrease in the value of the apparent dissociation constant K_{d2}. To maintain the physiologic relevance, the negative charge on the lipid was never increased above 30% in our experiments. Within these limits, the strength of the interaction was directly proportional to the density of the negative charge on the surface of the lipid vesicles

(Figure 1). The interaction is unaffected by changing the chemical nature of the negative charge, such as replacing PG with PS (data not shown), but it is attenuated in the presence of a high salt concentration (Figure 4). The fluorescence anisotropy of tryptophan, another measure of binding, also showed a greater increase with an increase in the negative charge in the membrane (Figure 8). Our data thus confirm that electrostatic forces between the basic peptide TAT-PTD and negative charges on phospholipids play a major role in the membrane binding of the peptide. However, nonelectrostatic forces cannot be neglected in binding of TAT-PTD to the membrane. They contribute ~24% to the extent of binding, as revealed by the presence of a phase that was unaffected by high salt and also appeared in the binding to membranes composed of pure neutral lipids. This phase of binding represents an irreversible step in the interaction, since the high salt concentration added after TAT-PTD had bound did not cause the peptide's dissociation from the membrane. Our fluorescence-derived binding isotherms compare very well with those obtained by Ziegler et al. (*32*) by isothermal titration calorimetry. The latter authors explained their data in terms of Gouy−Chapman theory and concluded that electrostatics account for 77% of the binding, which we confirm herein. The value of the apparent dissociation constant for this process, 610 μM, also agrees well with their overall binding constant K_{app}, ranging between 10^3 and 10^4 M^{-1}.

The peak of the tryptopan fluorescence emission was at 360 nm, and its position did not change upon the addition of lipid, regardless of the presence or absence of negative charge in the bilayer. This indicates that the N-terminal tryptophan remains in the polar aqueous environment even upon binding to the membrane, which was confirmed by the ability of acrylamide to completely quench the tryptophan fluorescence of the membrane-bound peptide (Figure 7).

Interaction with the DMPC/DMPG (3:1) membrane caused significantly greater changes in fluorescence of TAT-PTD when the membrane was in the liquid-crystal state, above its transition temperature (Figure 3). This indicates that the selective aggregation of negatively charged lipids by the cationic TAT-PTD peptide, implicitly assumed in the work of Ziegler et al. (*32*) and others, is required for strong binding to the membrane. We tested this directly in experiments with pyrene-labeled PG, which exhibits excimer fluorescence when the fluorophores are sufficiently close to each other. A greater than 100% increase in the excimer:monomer ratio was observed in the DMPC/DMPG membrane in the liquid-crystal state. These experiments demonstrate that, apart from the presence of negative charge, membrane fluidity is another important determinant for efficient binding of TAT-PTD to the membrane. On the other hand, these results suggest that binding of TAT-PTD may alter the physicochemical properties of the membrane; namely, it may cause phase separation of lipids into distinct microdomains. A change in membrane properties upon binding of another cationic peptide was recently suggested by Hitz et al. (*50*).

Membrane potential studies were carried out to determine, first, if TAT-PTD binding perturbs the membrane to a significant extent so that ions can leak through and, second, if the membrane potential (negative inside), inherently seen in the living cells, can assist cationic peptides in crossing the high-energy barrier during their internalization. Our data show no dissipation of membrane potential induced by TAT-PTD, whether it interacted with 100% egg PC LUV (data not shown) or with 3:1 egg PC/PG LUV (Figure 8) with a similar membrane potential. This contradicts the conclusion of Henriques et al. (*51*), who even called the presence of membrane potential the sine-qua-non condition for translocation of the synthetic CPP pep-1. The discord with our results may be due to, in part, the fact that their experiments were carried out with pep-1−β-galactosidase complexes rather than the naked peptide; the nature of their test for translocation, which was based on protection of β-galactosidase from digestion by trypsin applied from the cis side; and, most obviously, the different chemical nature of the peptide (pep-1 carries a smaller positive charge at neutral pH but is much more hydrophobic than TAT-PTD). Ziegler et al. (*32*) reported that TAT-PTD did not induce leakage of entrapped calcein (molecular mass of 623 Da) from lipid vesicles, and we extend that conclusion to the case of small ions; even temporary opening of passageways for ions would manifest in membrane potential dissipation. We also tested if the presence of membrane potential affects binding of TAT-PTD to the membrane. The limited stability of membrane potential in vesicles precludes determination of the apparent dissociation constant from titration experiments; hence, we monitored the fluorescence of only the bound peptide before and after establishing the membrane potential. We observed no change in intensity or wavelength shift, which indicates that membrane potential does not appreciably influence the manner in which TAT-PTD binds to the membrane.

Insertion of TAT-PTD into the Membrane. From the measured efficiency of FRET, we calculated the distance between the N-terminal tryptophan on the bound TAT-PTD and the membrane probe TMA-DPH as 3.4 nm. The charged head group of TMA-DPH anchors the probe at the membrane−water interface, oriented in parallel with the phospholipid acyl chains. Considering that there is only one neutral amino acid (glycine) between the terminal tryptophan and the first positively charged amino acid residue (arginine), the large distance is surprising. A possible explanation might be that the positively charged TMA-DPH was repelled by the positive charges on the peptide (the nearby N-terminus and the cluster of basic amino acid residues), and consequently, the measured distance is not the expected shortest distance between the two fluorophores along the normal to the membrane (i.e., with the probe located directly under the peptide's tryptophan). There was no observable FRET between the tryptophan and the uncharged hydrophobic probe DPH, which partitions predominantly in the hydrophobic core of the lipid bilayer. This indicates that the distance from the tryptophan to DPH is larger than that to TMA-DPH. These data, in conjunction with the quenching data, allow us to conclude that the N-terminus of TAT-PTD does not insert into the lipid bilayer. The value of fluorescence anisotropy of neither TMA-DPH nor DPH was affected by TAT-PTD binding, which indicates that TAT-PTD does not have any effect on the fluidity of the lipid bilayer. Hitz et al. (*50*) very recently reported rigidification of the PC/PG bilayer by oligoarginines, based on the peptide-induced decrease in the excimer:monomer ratio of pyrene-PG. It is hard to explain the peptide-induced increase in pyrene monomer fluorescence observed in that work. We saw just the opposite: upon

interaction with the basic peptide, the monomer fluorescence decreased because the energy was rather emitted by excimers, whose fluorescence increased concomitantly, due to sequestration of the negatively charged pyrene-PG by the basic peptide. We prefer this interpretation to the alternative of an increase in membrane fluidity because the latter was ruled out by our DPH fluorescence anisotropy data. Several factors may contribute to the difference between our conclusion and that of Hitz et al., including their use of LUV vs our SUV and, perhaps even more significantly, the very high concentration of PG (70%) in their membranes: the much more abundant unlabeled PG might have excluded the pyrene-PG from significant binding and sequestration that would manifest itself as an increase in the excimer:monomer fluorescence ratio. At any rate, the lack of a peptide effect on overall membrane fluidity, which we observed, suggests that no portion of TAT-PDH is inserted into the bilayer. If it did, one would expect an increase in the anisotropy values, particularly that of TMA-DPH, as a consequence of an increase in surface pressure and a decrease in free volume in the membrane after peptide insertion. It is worth noting that Ziegler et al. (*32*) also reported that TAT-PTD did not insert into a lipid monolayer at surface pressures that are close to the physiologic pressure.

Conclusion. Our data support the conclusion reached previously by others that electrostatic forces have a major role in the initial interaction of TAT-PTD with the lipid bilayer. In a physiologic range, the strength of the interaction was directly proportional to the density of negative charge in the membrane. However, there is a second, irreversible, phase in the binding, which is attributed to nonelectrostatic forces, such as hydrogen bonding and hydrophobic or van der Waals forces. It is possible that a conformational change in the peptide during the interaction makes a thermodynamic contribution to this step. The peptide binding does not compromise the integrity of the lipid bilayer and does not perturb the latter in any significant degree, so molecules or ions do not leak from vesicles. An important new result of ours is that the efficient binding of TAT-PTD requires a fluid membrane with lipids in the liquid-crystal state. We explain this requirement in terms of the peptide-induced selective segregation of the negatively charged lipids, which is necessary to neutralize the positive charges on the peptide. However, this does not imply formation of separate large macrodomains of negatively charged lipids within the membrane. Although the actual internalization of the cationic protein transduction domain was not directly addressed in our experiments, our data support the cautious conclusions of Ziegler et al. (*32*) and Richard et al. (*6*), namely, that no evidence of peptide translocation is apparent in our model system.

REFERENCES

1. Frankel, A. D., and Pabo, C. O. (1988) Cellular uptake of the tat protein from human immunodeficiency virus, *Cell 55*, 1189−1193.
2. Green, M., and Loewenstein, P. M. (1988) Autonomous functional domains of chemically synthesized human immunodeficiency virus tat trans-activator protein, *Cell 55*, 1179−1188.
3. Joliot, A., Pernelle, C., Deagostini-Bazin, H., and Prochiantz, A. (1991) Antennapedia homeobox peptide regulates neural morphogenesis, *Proc. Natl. Acad. Sci. U.S.A. 88*, 1864−1868.
4. Derossi, D., Joliot, A. H., Chassaing, G., and Prochiantz, A. (1994) The third helix of the Antennapedia homeodomain translocates through biological membranes, *J. Biol. Chem. 269*, 10444−10450.
5. Elliott, G., and O'Hare, P. (1997) Intercellular trafficking and protein delivery by a herpesvirus structural protein, *Cell 88*, 223−233.
6. Richard, J. P., Melikov, K., Vives, E., Ramos, C., Verbeure, B., Gait, M. J., Chernomordik, L. V., and Lebleu, B. (2003) Cell-penetrating peptides. A reevaluation of the mechanism of cellular uptake, *J. Biol. Chem. 278*, 585−590.
7. Derossi, D., Chassaing, G., and Prochiantz, A. (1998) Trojan peptides: The penetratin system for intracellular delivery, *Trends Cell Biol. 8*, 84−87.
8. Lindgren, M., Hallbrink, M., Prochiantz, A., and Langel, U. (2000) Cell-penetrating peptides, *Trends Pharmacol. Sci. 21*, 99−103.
9. Schwarze, S. R., Hruska, K. A., and Dowdy, S. F. (2000) Protein transduction: Unrestricted delivery into all cells? *Trends Cell Biol. 10*, 290−295.
10. Ziegler, A., Nervi, P., Durrenberger, M., and Seelig, J. (2005) The cationic cell-penetrating peptide CPP(TAT) derived from the HIV-1 protein TAT is rapidly transported into living fibroblasts: Optical, biophysical, and metabolic evidence, *Biochemistry 44*, 138−148.
11. Zorko, M., and Langel, U. (2005) Cell-penetrating peptides: Mechanism and kinetics of cargo delivery, *Adv. Drug Delivery Rev. 57*, 529−545.
12. Pooga, M., Hallbrink, M., Zorko, M., and Langel, U. (1998) Cell penetration by transportan, *FASEB J. 12*, 67−77.
13. Futaki, S., Goto, S., Suzuki, T., Nakase, I., and Sugiura, Y. (2003) Structural variety of membrane permeable peptides, *Curr. Protein Pept. Sci. 4*, 87−96.
14. Vives, E., Brodin, P., and Lebleu, B. (1997) A truncated HIV-1 Tat protein basic domain rapidly translocates through the plasma membrane and accumulates in the cell nucleus, *J. Biol. Chem. 272*, 16010−16017.
15. Scheller, A., Oehlke, J., Wiesner, B., Dathe, M., Krause, E., Beyermann, M., Melzig, M., and Bienert, M. (1999) Structural requirements for cellular uptake of α-helical amphipathic peptides, *J. Pept. Sci. 5*, 185−194.
16. Perez, J. L., De Ona, M., Niubo, J., Villar, H., Melon, S., Garcia, A., and Martin, R. (1995) Comparison of several fixation methods for cytomegalovirus antigenemia assay, *J. Clin. Microbiol. 33*, 1646−1649.
17. DiDonato, D., and Brasaemle, D. L. (2003) Fixation methods for the study of lipid droplets by immunofluorescence microscopy, *J. Histochem. Cytochem. 51*, 773−780.
18. Derossi, D., Calvet, S., Trembleau, A., Brunissen, A., Chassaing, G., and Prochiantz, A. (1996) Cell internalization of the third helix of the Antennapedia homeodomain is receptor-independent, *J. Biol. Chem. 271*, 18188−18193.
19. Mitchell, D. J., Kim, D. T., Steinman, L., Fathman, C. G., and Rothbard, J. B. (2000) Polyarginine enters cells more efficiently than other polycationic homopolymers, *J. Pept. Res. 56*, 318−325.
20. Futaki, S., Suzuki, T., Ohashi, W., Yagami, T., Tanaka, S., Ueda, K., and Sugiura, Y. (2001) Arginine-rich peptides. An abundant source of membrane-permeable peptides having potential as carriers for intracellular protein delivery, *J. Biol. Chem. 276*, 5836−5840.
21. Schwarze, S. R., Ho, A., Vocero-Akbani, A., and Dowdy, S. F. (1999) In vivo protein transduction: Delivery of a biologically active protein into the mouse, *Science 285*, 1569−1572.
22. Vives, E., Richard, J. P., Rispal, C., and Lebleu, B. (2003) TAT peptide internalization: Seeking the mechanism of entry, *Curr. Protein Pept. Sci. 4*, 125−132.
23. Kaplan, I. M., Wadia, J. S., and Dowdy, S. F. (2005) Cationic TAT peptide transduction domain enters cells by macropinocytosis, *J. Controlled Release 102*, 247−253.
24. Oehlke, J., Scheller, A., Wiesner, B., Krause, E., Beyermann, M., Klauschenz, E., Melzig, M., and Bienert, M. (1998) Cellular uptake of an α-helical amphipathic model peptide with the potential to deliver polar compounds into the cell interior non-endocytically, *Biochim. Biophys. Acta 1414*, 127−139.
25. Thoren, P. E., Persson, D., Karlsson, M., and Norden, B. (2000) The antennapedia peptide penetratin translocates across lipid bilayers: The first direct observation, *FEBS Lett. 482*, 265−268.
26. Lundberg, P., and Langel, U. (2003) A brief introduction to cell-penetrating peptides, *J. Mol. Recognit. 16*, 227−233.
27. Ziady, A. G., Ferkol, T., Gerken, T., Dawson, D. V., Perlmutter, D. H., and Davis, P. B. (1998) Ligand substitution of receptor targeted DNA complexes affects gene transfer into hepatoma cells, *Gene Ther. 5*, 1685−1697.

28. Swedlow, J. R., Hu, K., Andrews, P. D., Roos, D. S., and Murray, J. M. (2002) Measuring tubulin content in *Toxoplasma gondii*: A comparison of laser-scanning confocal and wide-field fluorescence microscopy, *Proc. Natl. Acad. Sci. U.S.A. 99*, 2014−2019.
29. Wadia, J. S., and Dowdy, S. F. (2002) Protein transduction technology, *Curr. Opin. Biotechnol. 13*, 52−56.
30. Bhatnagar, A., Sheffler, D. J., Kroeze, W. K., Compton-Toth, B., and Roth, B. L. (2004) Caveolin-1 interacts with 5-HT2A serotonin receptors and profoundly modulates the signaling of selected Gαq-coupled protein receptors, *J. Biol. Chem. 279*, 34614−34623.
31. Sodroski, J., Patarca, R., Rosen, C., Wong-Staal, F., and Haseltine, W. (1985) Location of the trans-activating region on the genome of human T-cell lymphotropic virus type III, *Science 229*, 74−77.
32. Ziegler, A., Blatter, X. L., Seelig, A., and Seelig, J. (2003) Protein transduction domains of HIV-1 and SIV TAT interact with charged lipid vesicles. Binding mechanism and thermodynamic analysis, *Biochemistry 42*, 9185−9194.
33. Tyagi, M., Rusnati, M., Presta, M., and Giacca, M. (2001) Internalization of HIV-1 tat requires cell surface heparan sulfate proteoglycans, *J. Biol. Chem. 276*, 3254−3261.
34. Sandgren, S., Cheng, F., and Belting, M. (2002) Nuclear targeting of macromolecular polyanions by an HIV-Tat derived peptide. Role for cell-surface proteoglycans, *J. Biol. Chem. 277*, 38877−38883.
35. Butko, P., Huang, F., Pusztai-Carey, M., and Surewicz, W. K. (1996) Membrane permeabilization induced by cytolytic δ-endotoxin CytA from *Bacillus thuringiensis* var. *israelensis*, *Biochemistry 35*, 11355−11360.
36. MacDonald, R. C., MacDonald, R. I., Menco, B. P., Takeshita, K., Subbarao, N. K., and Hu, L. R. (1991) Small-volume extrusion apparatus for preparation of large, unilamellar vesicles, *Biochim. Biophys. Acta 1061*, 297−303.
37. van Der Meer, B. W., Coker, I. G., and Chen, S.-Y. S. (1994) *Resonance Energy Transfer Theory and Data*, VCH Publishers, Inc., New York.
38. Eftink, M. R., and Ghiron, C. A. (1976) Exposure of tryptophanyl residues in proteins. Quantitative determination by fluorescence quenching studies, *Biochemistry 15*, 672−680.
39. Manceva, S. D., Pusztai-Carey, M., and Butko, P. (2004) Effect of pH and ionic strength on the cytolytic toxin Cyt1A: A fluorescence spectroscopy study, *Biochim. Biophys. Acta 1699*, 123−130.
40. Yamamoto, T., Tachikawa, A., Terauchi, S., Yamashita, K., Kataoka, M., Terada, H., and Shinohara, Y. (2004) Multiple effects of DiS-C_3(5) on mitochondrial structure and function, *Eur. J. Biochem. 271*, 3573−3579.
41. van Holde, K. E., Johnson, W. C., and Ho, P. S. (1998) *Principles of Physical Biochmeistry*, 2nd ed., Prentice Hall, Upper Saddle River, NJ.
42. Mason, J. T. (1998) Investigation of phase transitions in bilayer membranes, *Methods Enzymol. 295*, 468−494.
43. Needham, D., McIntosh, T. J., and Evans, E. (1988) Thermomechanical and transition properties of dimyristoylphosphatidylcholine/cholesterol bilayers, *Biochemistry 27*, 4668−4673.
44. Caputo, G. A., and London, E. (2003) Using a novel dual fluorescence quenching assay for measurement of tryptophan depth within lipid bilayers to determine hydrophobic α-helix locations within membranes, *Biochemistry 42*, 3265−3274.
45. Vogel, B. E., Lee, S. J., Hildebrand, A., Craig, W., Pierschbacher, M. D., Wong-Staal, F., and Ruoslahti, E. (1993) A novel integrin specificity exemplified by binding of the αvβ5 integrin to the basic domain of the HIV Tat protein and vitronectin, *J. Cell Biol. 121*, 461−468.
46. Weeks, B. S., Desai, K., Loewenstein, P. M., Klotman, M. E., Klotman, P. E., Green, M., and Kleinman, H. K. (1993) Identification of a novel cell attachment domain in the HIV-1 Tat protein and its 90-kDa cell surface binding protein, *J. Biol. Chem. 268*, 5279−5284.
47. Ziegler, A., and Seelig, J. (2004) Interaction of the protein transduction domain of HIV-1 TAT with heparan sulfate: Binding mechanism and thermodynamic parameters, *Biophys. J. 86*, 254−263.
48. Silhol, M., Tyagi, M., Giacca, M., Lebleu, B., and Vives, E. (2002) Different mechanisms for cellular internalization of the HIV-1 Tat-derived cell penetrating peptide and recombinant proteins fused to Tat, *Eur. J. Biochem. 269*, 494−501.
49. Richard, J. P., Melikov, K., Brooks, H., Prevot, P., Lebleu, B., and Chernomordik, L. V. (2005) Cellular uptake of unconjugated TAT peptide involves clathrin-dependent endocytosis and heparan sulfate receptors, *J. Biol. Chem. 280*, 15300−15306.
50. Hitz, T., Iten, R., Gardiner, J., Namoto, K., Walde, P., and Seebach, D. (2006) Interaction of α- and β-oligoarginine acids and amides with anionic lipid vesicles: A mechanistic and thermodynamic study, *Biochemistry 45*, 5817−5829.
51. Henriques, S. T., Costa, J., and Castanho, M. A. (2005) Translocation of β-galactosidase mediated by the cell-penetrating peptide pep-1 into lipid vesicles and human HeLa cells is driven by membrane electrostatic potential, *Biochemistry 44*, 10189−10198.

BI602527T